EXAFS AND XRD STUDIES OF ‘ZN-CO’ ALLOY ELECTRODEPOSITS

D.E.O.S. CARPENTER[1,2], S.D. CARPENTER[1,2].

[1] Blumenau University, FURB, Santa Catarina, Brazil
[2] Birmingham University, Birmingham, UK
E-mail para contato: carpenter@furb.br

ABSTRACT – The sacrificial behaviour of electrodeposited zinc layer on the surface of a ferrous alloy to delay the onset of ferrous corrosion is very well documented in the literature. However zinc-cobalt alloys show a marked improvement in the corrosion protection of a ferrous substrate in comparison with pure zinc layers. A protective layer of zinc-cobalt can be applied by means of simultaneous electro-deposition. The electro-deposited structure of a zinc-cobalt alloy was studied using X-Ray Diffraction (XRD) and Extended X-ray Absorption Fine Structure (EXAFS). The morphology of the electro-deposit was found to be significantly dependant on cobalt concentration of the electrolyte. Dilute electrolytes were found to yield a single phase hexagonal close packed (hcp) deposit similar to that of the constituent metals themselves. However electro-deposits formed under the same condition from electrolytes of higher cobalt concentration were found to contain a fine dispersion of an intermetallic phase identified as ‘Co_5Zn_{21}’.

1. INTRODUCTION

Electrochemical processes are well established within the metals finishing industry and have a broad range commercial importance; e.g. surface aesthetics, hard surface coatings, corrosion protection and the incorporation of electro-magnetic layers onto devices etc. Although the enhancement of a single property within an electro-deposit is highly prized the enhancement and control of several properties is of much greater interest. The majority of electro-deposited alloys of commercial interest are single phase solid solutions (Weil, 1992). However several electro deposited binary alloys, e.g. Zn-Fe, Zn-Ni and Cu-Cd alloys, containing more than one phase are reported in the literature (Despic *et al*, 1989; Swarthirajan, 1987; Drewien *et al*, 1996). The Zinc-Cobalt thermal equilibrium diagram is particularly complex at higher zinc concentrations and closely resembles the diagrams for Zinc-Iron and Zinc-Nickel. However it is important to realize that electro-deposited alloys are non-equilibrium and may undergo stress relief when heated to relatively low temperature. The key variables that determine the phase constitution of an electro-deposited alloy are electrolyte composition, electrolyte agitation, temperature and current density at the cathode, (Swarthirajan, 1987).

The main objective was to ascertain the precise crystalline nature and atomic arrangement within a zinc-cobalt alloy electro-deposits under investigation.

2. EXPERIMENTAL

2.1. Sample Preparation

The Zn-Co electrodeposits were obtained from the electrolytes presented in the Table 1.

Table 1 - Chemical composition of (**a**) alkaline electrolytes ‘A’ and ‘B’ and (**b**) acid electrolyte

(**a**)

Constituents	**Concentration g.dm^{-3}**	
	Electolyte ‘**A**’	Electrolyte ‘**B**’
ZnO	10	10
NaOH	100	100
$CoSO_4 . H_2O$	4	64
Triethanolamine	6	92
‘Zn/Co’ Ratio	7.05	0.83

(**b**)

Constituents	**Concentration g.dm^{-3}**
	Electolyte ‘**C**’
$ZnSO_4$	44
$CoSO_4 . H_2O$	48
H_3BO_3	10
$(NH_4)_2SO_4$	50
‘Zn/Co’ Ratio	0.99

. The substrate of 0.1 % carbon steel was ground to a 1200 ‘grit’ surface finish and degreased. The residual oxide films on the surface of the electrodes were removed by immersion into a 25 % v/v solution of sulphuric acid in distilled water. This was followed by a distilled water rinse and dry using hot air blower.

The electrolytic cell conditions were 2.5 Adm^{-2} at room temperature without agitation. The duration selected for the electrolysis was 30 minutes for the alkaline electrolytes ‘A’ and ‘B’ and 60 minutes for the acid electrolyte ‘C’ to give a deposit thickness in the region of 15 μm.

2.2. X-ray Diffraction

X-ray diffraction was carried out on all of the electro-deposited ‘Zn-Co’ samples using a ‘PW diffractometer’ using ‘Cuk radiation (0.1542 nm). ‘Grazing Incidence Angle’ diffraction studies were also undertaken at ‘Station 2.3’ of the Syncrotron Radiation Source (SRS) at Daresbury Analytical Research and Technology Service UK (DART). The Grazing incident angle method was used so as to minimise the contribution of the substrate electrode to the diffraction information obtained from the ‘Zn-Co’ electro-deposit.

2.3. EXAFS

EXAFS was performed using the (111) plane of a silicon crystal as a monochromator to ‘tune’ the x-ray energy of the cobalt ‘k-edge’. The monochromator was ‘detuned’ to reject 20 % and minimise the harmonic content of the signal. The dimensions of the x-ray beam incident on the samples were determined by the pre and post monochromator slit adjustments.

The monochromator angle for cobalt was calibrated by running an ‘edge scan’ on a 5µm thick foil of cobalt and found to be 17.5°.

3. RESULTS AND DISCUSSION

Figures 1 (a), (b) and (c) show the x-ray spectrometer scans for the electro-deposits obtained from electrolyte ‘A’, ‘B’ and ‘C’ respectively. The individual peaks corresponding to the family of atomic planes for each crystalline phase are numbered and are identified within the Table associated with each Figure. Please note that the ‘zinc’ phase is actually a solid solution of cobalt in zinc and that the indices for this phase are as for the hexagonal system of coordinates.

Figure 1(a) shows that the deposit obtained from the alkaline solution containing 4 grams of cobalt per litre is a binary solid solution of cobalt in zinc. The spectrometer scan shows that the electro-deposit also contains a small amount of cobalt hydroxide.

Figure 1(b) shows that the deposit obtained from the alkaline solution containing 64 grams of cobalt per litre is also a solid solution of cobalt in zinc. The spectrometer scan also shows that there are two different oxides of cobalt ‘CoO’ and ‘Co_3O_4’ within the electro-deposit plus two associated hydroxides ‘CoOOH’ and ‘$Co(OH)_2$’. This is associated with the higher concentration of metallic cobalt dissolved within the zinc electro-deposit. It is interesting to note that two higher order reflections for the intermetallic compound ‘Co_5Zn_{21}’ also appear in the spectrometer scan.

Figure 1(c) shows the x-ray spectrometer scan from the deposit obtained from the acid solution containing 48 grams of cobalt per litre. It is interesting to note that this deposit also contains a small amount of ‘CoOOH’ because of the higher concentration of cobalt within the electro-deposit. More significantly the higher concentration of cobalt has resulted in the formation of ‘Co_5Zn_{21}’ in a similar way as for the alkaline electrolyte ‘C’.

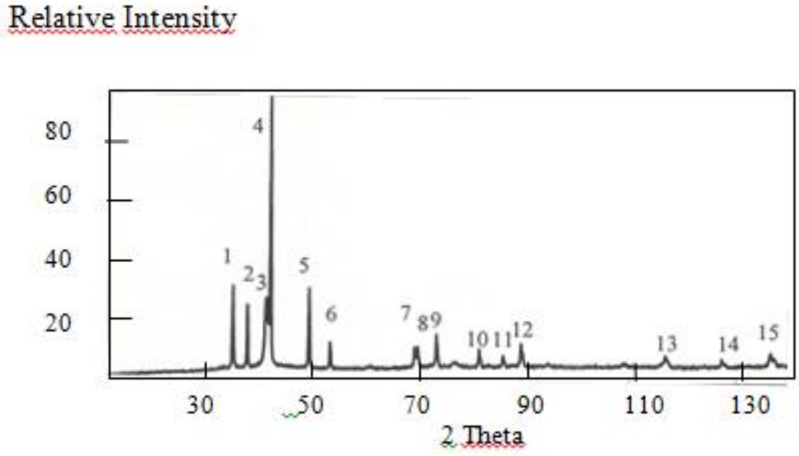

Peak No.	Plane {hk(i)l}.	Phase.
1	002	Zn
2	100	Zn
3	121	CoOOH
4	101	Zn
5	200	Cu
6	102	Zn
7	103	Zn
8	110	Zn
9	220	Cu
10	112	Zn
11	201	Zn
12	104	Zn
13	400	Cu
14	211	Zn
15	331	Cu

Figure 1(a) - X-ray spectrometer scan and peak identification for the Electro-deposit obtained from Electrolyte ‘A’.

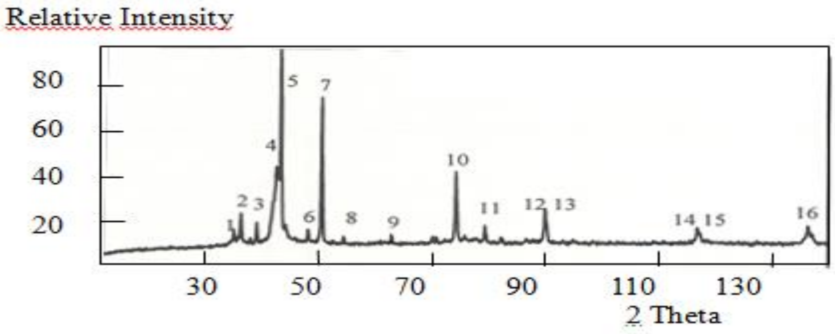

Peak No.	Plane {hk(i)l}.	Phase
1	130	CoOOH
2	002	Zn
3	012	CoOOH
4	200	CoO
5	101	Zn
6	131	CoOOH
7	200	Cu
8	532	$CoZn_{13}$
9		ZnO
10	220	Cu
11	642	Co_5Zn_{21}
12	733	Co_5Zn_{21}
13	311	Cu
14	114	Zn
15	400	Cu
16	331	Cu

Figure 1(b) - X-ray spectrometer scan and peak identification for the Electro-deposit obtained from Electrolyte 'B'.

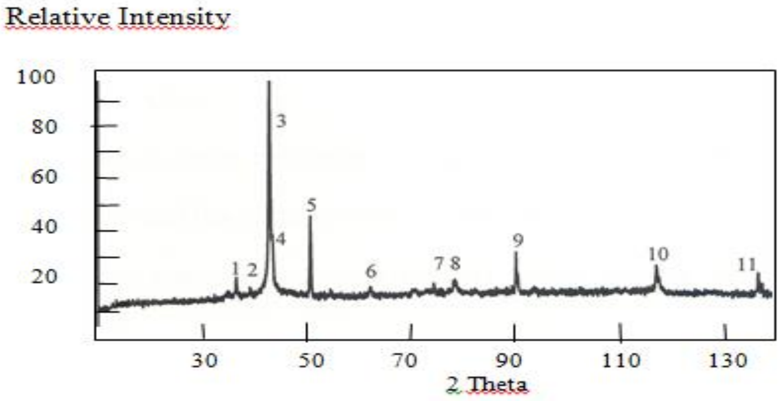

Peak No.	Plane {hk(i)l}.	Phase
1	002	Zn
2	100	Zn
3	101	Zn
4	111	Cu
5	200	Cu
6	015	CoOOH
7	107	CoOOH
8	550	Co_5Zn_{21}
9	721	Co_5Zn_{21}
10	331	Cu
11	400	Zn

Figure 1(c) - X-ray spectrometer scan and peak identification for the Electro-deposit obtained from Electrolyte 'C'.

Table 2 shows how the 'c/a' ratio of the hexagonal unit cell of the electro-deposited was found to vary with cobalt content.

Table 2 - Variation of 'c/a' ratio of the hexagonal unit cell with cobalt content of the 'Zn-Co' electro-deposit

Electrolyte	**'Co' content in alloy**	**'c/a' ratio (angstroms)**
'**A**'	3.34 wt%	1.858
-	4.86 wt%	1.86
-	6.93 wt%	1.86
-	8.18 wt%	1.863
'**B**'	12.41 wt%	1.861
'**C**'	17.07 wt%	1.826
Pure zinc	0.00 wt%	1.85

The trend in the ‘c/a’ values indicate that the ‘c/a’ ratio increases with increasing cobalt content. This would suggest, in accordance with Vegard’s law, that the lattice parameter ‘a’ decreases as a consequence of the slightly smaller metallic radius (0.125 nm) of the cobalt atom in comparison to the radius (0.138 nm) of the zinc atom. Interestingly there is a 2 % increase in the size of the unit cell for the ‘Zn-Co’ solid solution containing 12 weight % cobalt (Electrolye ‘C’) in comparison to that of pure zinc, Table 3. Therefore this would also suggest that the average lattice parameter ‘c’ is also influenced by the percentage of cobalt atoms within the solid solution.

Table 3 - Variation of unit cell size with cobalt content and phase constitution of electro deposit.

Electrolyte	**‘Unit cell’ volume of deposit**	**Phase constituents**
‘A’	**30.329**	**‘η’**
‘B’	**31.096**	**‘η’ + ‘Γ’**
‘C’	**31.136**	**‘η’ + ‘Γ’**
Pure zinc	**30.434**	**‘η’**

Figure 2(a) shows and compares the ‘fine structure’ data obtained from the ‘EXAFS’ experiments for the electro-deposits obtained from electrolytes ‘B’ and ‘C’ when the Synchrotron radiation source was tuned to the ‘k’ absorption edge of cobalt. Similarly Figure 2(b) shows and compares the data acquired from the deposits obtained from electrolytes ‘A’ and ‘C’. Both Figure 2(a) and (b) show the corresponding Fourier transforms and both Figures fit with the theoretical transforms obtained for high concentrations and low concentrations of cobalt respectively (Figures 3 and 4). The scattering amplitude (K^2) shown in Figure 2(b) for the electro deposit obtained from electrolyte ‘A’ is greater than that obtained from electrolyte ‘B’ across the entire range of the waveform. However both the waveforms shown in Figures 2(a) and (b) are in complete phase and only one significant peak is shown within the corresponding Fourier transforms. The single peak of the transform clearly shows that the average atomic distance between an individual cobalt atom and all of its nearest neighbours within the close packed hexagonal unit cell is 2.5 (±0.02) angstroms. The ‘fitted’ waveform and corresponding Fourier transform shown in Figures 3 and 4 also indicate that there is a high probability that all the cobalt atoms within the hexagonal crystal lattice are isolated and only have zinc atoms as neighbours.

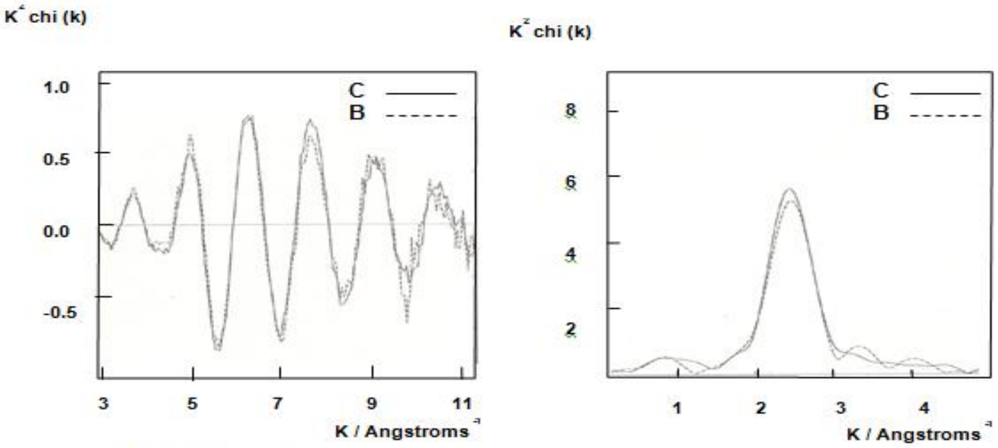

EXAFS spectra

Fourier transform

Figure 2(a). Comparison of ‘EXAFS’ spectra and Fourier transforms for the electro-deposit obtained from electrolytes ‘B’ and ‘C’.

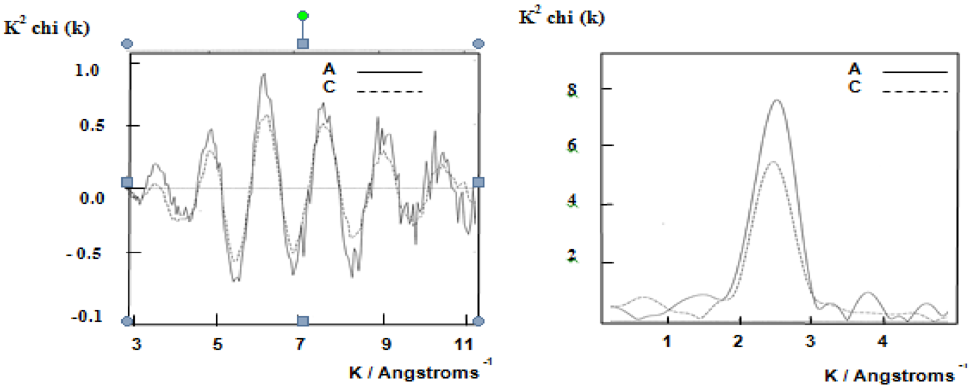

EXAFS spectra

Fourier transform

Figure 2(b) - Comparison of ‘EXAFS’ spectra and Fourier transforms for the electro-deposit obtained from electrolytes ‘A’ and ‘C’.

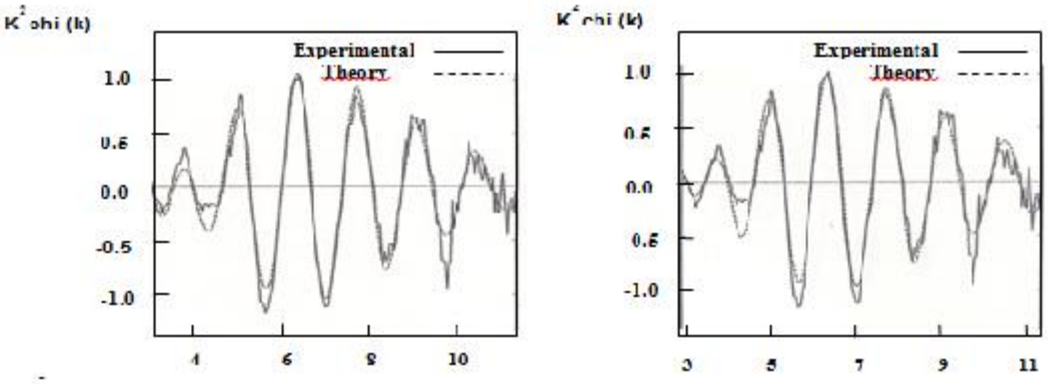

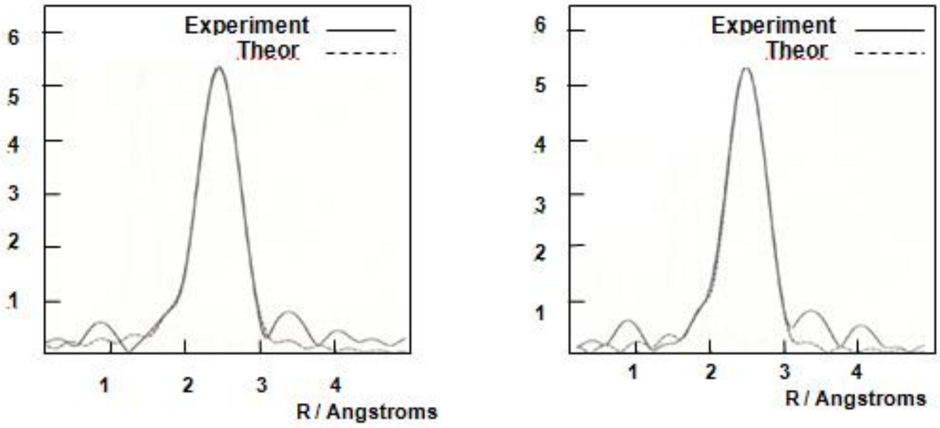

Figure 3 - Data fit for the samples obtained from Electrolyte 'B' showing the 'EXAFS' spectra and subsequent Fourier transforms below: **(a)** Simulation with 6 atoms of zinc as nearest neighbours and **(b)** simulation with 3.5 atoms of cobalt as nearest neighbours.

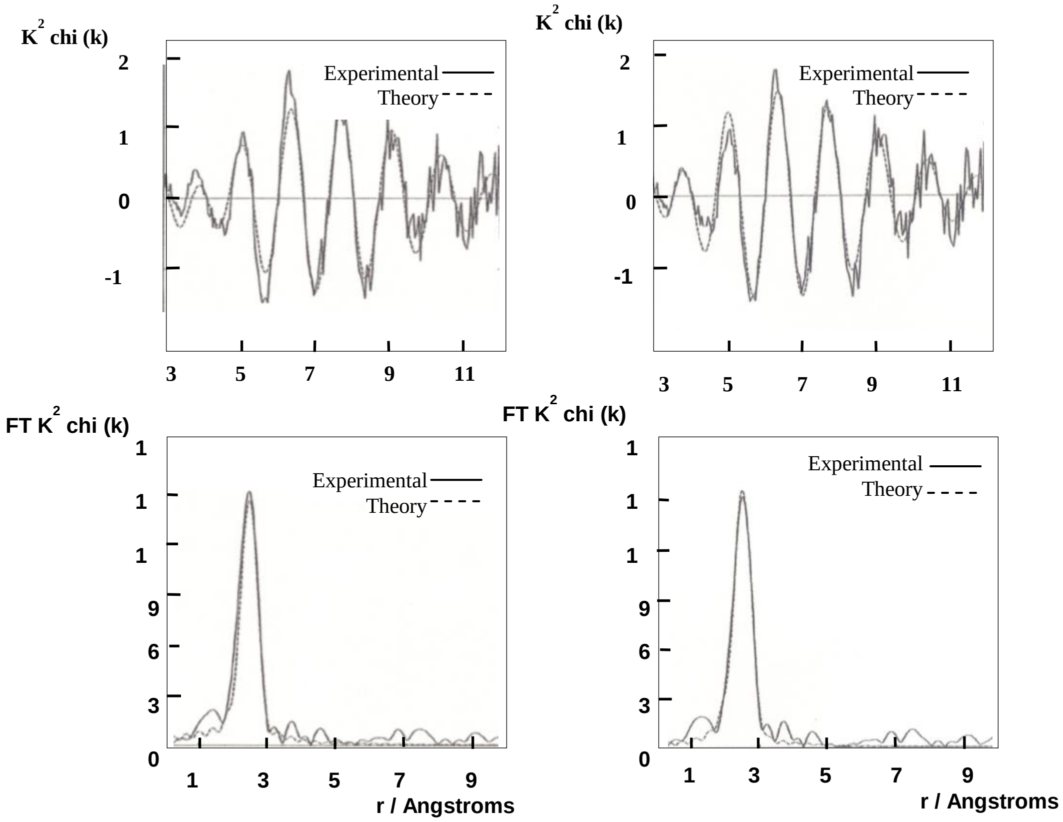

Figure 4 - Data fit for the sample obtained from electrolyte 'A' showing the 'EXAFS' spectra and subsequent Fourier transform below. (**a**) Simulation with atoms of zinc as nearest neighbours and (**b**) simulation with 6 atoms of cobalt as nearest neighbours.

Both zinc and cobalt have a hexagonal close packed (HCP) structure at ambient temperature and therefore have a certain 'miscibility' when in solid solution with each other

[Figure 1.]. This miscibility is also apparent within electro-alloys of zinc-cobalt whereby the 'Zn-Co' solid solution corresponds to the hexagonal equilibrium 'η' phase predicted at the low cobalt concentration end of the phase diagram, Table 1. The 'EXAFS' results indicate that the hexagonal non-equilibrium 'η' phase observed within electro-deposited "Zn-Co' alloys is a random solid solution and that no evidence ordering within the atomic lattice was observed during the diffraction experiments. This lack of evidence is further supported by electron diffraction undertaken during transmission electron microscopy experiments on similar electro-deposited alloys (Carpenter and Carpenter, 2000; Carpenter, 1999).

A more detailed examination of the 'EXAFS' spectra for the electro-deposit of lower cobalt concentration (Electrolyte 'A') revealed that the average inter atomic spacing between cobalt and the six neighbouring zinc atoms within the {0001} basal plane is 2.47 angstroms. This compares favourably with the 2.47 angstrom inter atomic spacing found between the zinc atoms within pure zinc. The inter atomic spacing was found to increase to 2.56 angstroms for higher cobalt concentrations (Electrolytes 'B' and 'C') and appears to be in contrast to Vegard's law. The deviation from Vegard's law is probably associated with the hybrid covalent bond that occur within a metallic crystal lattice and are responsible for the deviation away from the ideal 'c/a' ratio of 1.633 of a hexagonal close packed structure.

This present work also supports the findings by H. Kerstens, J. Godard et al, and H.L. Gaigher et al and indicates that 'Zn-Co' only deposits from an alkaline solution as a hexagonal close packed solid solution. However it must be noted that cobalt has been reported to deposit as an FCC structure from acid electrolyte (Kerntens, 1932; Godard and Wright, 1964; Gaigher, 1976).

Similarly to the 'Zn-Co' phase diagram (Figure 1.) the results show that there is a precipitation of an intermetallic compound (Co_5Zn_{21}) within electro-deposits of higher cobalt content (Table 2). This precipitate corresponds to the equilibrium 'Γ' phase found within the phase diagram.

With reference to the surface appearance of the 'Zn-Co' deposits (Figure 2) Crystal growth is favoured at relatively low 'over potentials' and the individual crystallites that form during the electro crystallization process coalesce into larger nodules. However the nucleation process demands a higher 'over potential' because of the greater amount of 'free energy' required to form a new surface. This 'free energy' can be supplied by local changes in the current density across the topography of the deposit. It is possible that the dendritic structures observed between the primary nodules of 'Zn-Co' are associated with these changes.

5. Conclusions

1. Zinc and cobalt codeposit as a hexagonal close packed random solid solution of cobalt in zinc when electro-deposited from an alkaline electrolyte containing up to 64 grams of cobalt ions per litre.

2. An alkaline electrolyte of 4 grams of cobalt ions per litre yields an electro-deposit containing ~3 wt % of cobalt in zinc and an alkaline electrolyte of 64 grams of cobalt ions per litre yields an electro deposit containing ~12 wt % of cobalt in zinc.

3. A dispersion of 'Co_5Zn_{21}' forms along with the hexagonal solid solution when the cobalt ion content of the electrolyte exceeds 48 grams per litre.

4. A dispersion of 'Co_5Zn_{21}' can form within the hexagonal solid solution from both acid and alkaline electrolytes.

Acknowledgements.

The authors would like to thank CAPES (Brazilian Government) for the sponsorship and to thank the CLRC laboratory at Daresbury UK for the use of there time and equipment at DART. The authors would also like to thank the University of Birmingham UK and University of Blumenau (FURB) for the use of their laboratory facilities.

6. References

CARPENTER, D.; CARPENTER, S. D.; FARR, J. P. G. Trans. IMF. 4, v. 78, p. 152, 2000.
CARPENTER, D.: Ph.D. Thesis, University of Birmingham, UK, 1999.
DESPIC, A.R.; JOVIC, V.D.; STEVANOVIC, J.S. S. Spaic, J. Electrochim. Acta. 34. p. 899, 1989.
DREWIEN,C.A.; GOLDSTEIN, J.I.; MARDER, A.R. Metallurgical and Metallurgical Transactions. 25 A, 6-7. 1041, 1996.
F.J.F. MIRANDA,F.J.F.; BARCIA, O.E.; Diaz, S. L.; MATTOS, O.R.; WIART, R. Electrochim. Acta. v. 41, p. 1119, 1996.
GODARD, J.; WRIGHT, J. G.; J. Applied Phys. v.15, p. 807, 1964.
H.L. GAIGHER, H.L.; VAN, N.G.; BERG, V.D. Electrochim. Acta. v. 21. p. 45, 1976.
KERSTENS, Physics, v. 2, p. 274, 1932.
SWARTHIRAJAN, S. J. Electroanal. Chem. 221. 211, 1987.